

*Letter to the Editor***Evidence for water ice and estimate of dust production rate in comet Hale-Bopp at 2.9 AU from the Sun***E. Lellouch¹, J. Crovisier¹, T. Lim^{2,3}, D. Bockelée-Morvan¹, K. Leech², M.S. Hanner⁴, B. Altieri², B. Schmitt⁵, F. Trotta⁵, and H.U. Keller⁶¹ Observatoire de Paris-Meudon, F-92195 Meudon, France² ISO Science Operations Centre, Astrophysics Division of ESA, Villafranca, Spain³ Queen Mary & Westfield College, University of London, London, UK⁴ Jet Propulsion Laboratory, Pasadena, CA 91109, USA⁵ Laboratoire de Glaciologie et Géophysique de l'Environnement, Saint Martin d'Hères, France⁶ MPI für Aeronomie, Postfach 20, D-37189 Katlenburg-Lindau, Germany

Received 2 July 1998 / Accepted 14 September 1998

Abstract. We report observational evidence for water ice in comet C/1995 O1 (Hale-Bopp) when it was at 2.9 AU from the Sun, from emission features at 44 and 65 μm , and possibly an absorption feature at 3.1 μm , observed with ISO/LWS and PHT. We find that icy grains have mean radii of 15 μm within a factor of 2, lifetimes of ~ 2 days, a temperature of ~ 153 K, and a total mass of $\sim 2 \times 10^9$ kg. From investigation of the continuum spectrum at 43–195 μm , we also infer a production rate of large particles (~ 100 μm) dust of about 4×10^4 kg s⁻¹.

Key words: comets: general – comet: individual: C/1995 O1 (Hale-Bopp) – infrared: solar system

1. Introduction

The possible existence of an *icy grain halo* around cometary nuclei has been debated for a long time. Indeed, icy particles are likely to be lifted off the nucleus along with refractory particles during cometary activity. At small heliocentric distances (r_h) such icy grains are expected to have short lifetimes and thus to be difficult to detect from ground-based observations (Hanner 1981). On the other hand, indirect evidences exist for the presence of icy grains at large r_h : for example, the production of water from some distant comets (A'Hearn et al. 1984), including C/1995 O1 (Hale-Bopp) (Biver et al. 1997), cannot be explained by free sublimation at the nucleus surface but rather from the sublimation of icy grains (Enzian et al. 1998; Prialnik 1998).

Send offprint requests to: J. Crovisier

* Based on observations with ISO, an ESA project with instruments funded by ESA Member States (especially the PI countries: France, Germany, the Netherlands and the United Kingdom) and with participation of ISAS and NASA.

Although previous searches for the water ice feature around 3.1 μm were inconclusive (e.g., in C/1983 O1 Černis; Hanner 1984a), water ice was detected in comet C/1995 O1 (Hale Bopp) at $r_h \sim 7$ AU from 1.50 and 2.04 μm absorption features (Davies et al. 1997). Other water ice features exist in the far-infrared at 44 and 65 μm . They have been observed in circumstellar shells (“Frosty Leo”; Omont et al. 1990), disks around young stars (HD 100546; Malfait et al. 1998), and protostars (e.g., RAFGL 7009S; Dartois et al. 1998).

We report here on observations of the 3.1, 44 and 65 μm water ice features in comet Hale-Bopp at $r_h = 2.9$ AU from the Sun using the Infrared Space Observatory (ISO). We also investigate the continuum spectrum at 43–195 μm to constrain the dust size and production rate of large particles.

2. Observations

The observations analyzed here were made on 26 September and 6 October 1996 as part of a comprehensive investigation of the infrared spectrum of comet Hale-Bopp with ISO (Crovisier et al. 1997a, 1997b). The full spectral scan (43–195 μm , spectral resolution $\lambda/\delta\lambda \sim 200$, field of view $\sim 100''$) obtained on 6 October with the Long Wavelength Spectrometer (LWS; Clegg et al. 1996) was re-reduced using the last version (7.0) of the standard pipeline (Fig. 1). The photometer grating spectrometer (PHT-S; Lemke et al. 1996) observed the 2.5–5 μm spectrum (spectral resolution $\lambda/\delta\lambda \sim 90$, field of view $24'' \times 24''$) on 26 September and 6 October.

3. Analysis*3.1. The LWS spectrum: water ice and dust emission*

Besides gaseous H₂O lines, the LWS spectrum shows two emissions, a narrow one centred at 44 μm , and another broader one, around 65 μm . Although the former is near the edge of the LWS

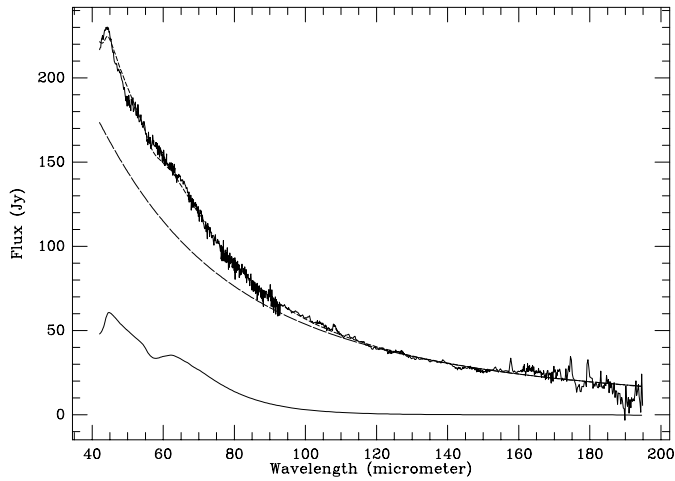


Fig. 1. LWS data along with model, obtained with ice particle radius $a = 15 \mu\text{m}$, ice temperature $T_s = 170\text{K}$, $T_{\text{dust}} = 210\text{K}$, $\beta = 0$ (see text). Solid line: contribution of the ice. Long-dashed line: contribution of the dust. Short-dashed line: sum of the two components. Several rotational lines of gaseous water are observed (and unmodelled) at 108, 175, 180 and (marginally) 101 μm

range, its reality is confirmed by the increase of flux at 41–44 μm in the ISO/SWS spectrum (see Crovisier et al. 1997a, 1997b). This structure is characteristic of crystalline water ice. Amorphous ice, with a broad band centred at 46 μm and no feature around 65 μm , does not match the spectrum. Crystalline olivine, identified on comet Hale-Bopp from its bands at 16–34 μm (Crovisier et al. 1997a), and pyroxene, detected at smaller r_h 's (Wooden et al. 1998), have structures beyond 40 μm (Koike et al. 1993; Koike & Shibai 1998; d'Hendecourt, *priv. comm.*), but the exact wavelengths do not match the observed emissions (e.g., forsterite has weak features at 50 and 70 μm). The ice bands appear superimposed on a continuum which is attributed to emission from cometary dust. To model the H_2O ice emissions, we used optical constants determined by Trotta (1996) from laboratory measurements of crystalline ice at 145 K. Extinction and absorption efficiencies (Q_{ext} and Q_{abs}) were calculated from Mie theory (van de Hulst 1957) for various grain sizes (radius a).

The thermal emission of an ice grain was modelled as $\phi(\lambda) = C_{\text{abs}}(\lambda)B(\lambda, T_s)$, where $C_{\text{abs}} = Q_{\text{abs}}\pi a^2$ and T_s is the temperature of sublimating ice grains. T_s values of 140 and 170 K were tested. The absolute contribution of the ice emission to the flux was inferred from the contrast of the bands above the estimated continuum. In practice, the LWS spectrum was fitted by the sum of an emission due to ice and of a continuum dust emission which was modelled either by a blackbody at temperature T_{dust} or by a blackbody multiplied by an emissivity proportional to $\lambda^{-\beta}$ (Jewitt & Matthews 1997). We did not consider radiative transfer effects (reabsorption) between different ice grains and between dust and ice. We therefore modelled the LWS spectrum in terms of five parameters: a , T_{dust} , the emissivity power index β , and the total emission cross sections for ice and dust (C_i and C_d).

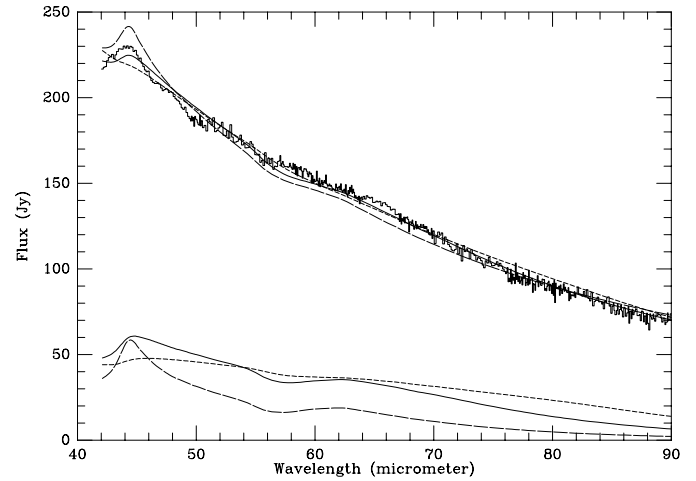


Fig. 2. The 40–90 μm region modelled with $T_s = 170\text{K}$ and different ice particle sizes. Solid line: $a = 15 \mu\text{m}$. Long-dashed line: $a = 7 \mu\text{m}$. Short-dashed line: $a = 30 \mu\text{m}$. The three bottom curves show the contribution of ice and the three top curves show attempts to fit the LWS data (histogram) with these three models

The particle radius was determined from the general shape of the 44 and 65 μm bands, in particular the relative contrast of the two bands. For $T_s = 170\text{K}$, the best fit was determined for $a = 15 \mu\text{m}$. Smaller particle sizes tend to produce too sharp a 44 μm band, while larger particles produce a general flattening of the spectrum which is not observed (Fig. 2). We consider that the particle size is determined within a factor of 2. One of the best overall fits to the data is shown in Fig. 1. At 44 μm , out of a total observed flux of $\sim 230\text{Jy}$, the ice emission contributes to about 60 Jy. This indicates a projected emitting area $C_i = 1.1 \times 10^5\text{km}^2$, i.e., an effective diameter of 375 km. This implies that water ice is seen in the coma and not on the nucleus. For $a = 15 \mu\text{m}$, this corresponds to about 1.5×10^{20} sublimating grains within the LWS beam (which corresponds to distances within $\sim 1.1 \times 10^5\text{km}$ from the nucleus), for a total ice mass of $M_{\text{ice}} = 1.9 \times 10^9\text{kg}$. Similar numbers are found for $T_s = 140\text{K}$: $a = 12 \mu\text{m}$, $C_i = 1.7 \times 10^5\text{km}^2$, $M_{\text{ice}} = 2.5 \times 10^9\text{kg}$.

In the best fit models, the flux due to dust is about 170 Jy at 44 μm . Beyond 100 μm , the observed flux must be entirely of dust origin. The dust spectrum can be well fitted with a blackbody at 210 K, similar to the colour temperature fitting the 2.9 AU SWS spectrum at 7.5 and 13–15 μm (Crovisier et al. 1997a) and $\sim 30\%$ above the equilibrium blackbody temperature ($T_{\text{BB}} \sim 165\text{K}$ at 2.9 AU). The elevated colour temperature, yet lack of steep decrease in the flux at long wavelengths, indicates a broad size distribution for the dust: model calculations for a power law size distribution a^{-n} of carbon grains in the range 0.1 μm to 1 cm suggests $n \leq 3.5$.

The roughly constant spectral emissivity from 100–200 μm (slope $\beta \sim 0$) contrasts with the millimetre/submillimetre region, where radiometric/interferometric data taken near perihelion indicate a spectrum much harder than a blackbody, with β ranging from 0.6 at $0.45 \leq \lambda \leq 2\text{mm}$ (Jewitt, *priv. comm.*) to 1.2 at 0.3–10 mm (Wink et al. 1998) and 1.39 at 1.4–2.1 mm

(Senay et al. 1998). This strong decrease in emissivity precludes a large contribution from dust particles larger than several hundred μm near perihelion, while $\beta \sim 0$ at 40–200 μm requires grains larger than 30 μm in radius. We adopt 100 μm as a typical grain size. This value is close to the maximum size of non-porous dust grains that can be lifted off a 70 km diameter (Weaver & Lamy 1998) nucleus given its activity at 2.9 AU ($\sim 2 \times 10^{29}$ CO molecules s^{-1} ; Biver et al. 1997) (e.g., Delsemme & Miller 1971).

The 100 μm flux (65 Jy) indicates a dust cross section of $C_d = 3.2 \times 10^5 \text{ km}^2$, i.e., an effective diameter of 640 km. Assuming $a = 100 \mu\text{m}$ and a density of 2.5 g cm^{-3} , this gives 10^{19} dust grains in the beam, for a total mass $M_{\text{dust}} = 1.1 \times 10^{11} \text{ kg}$. This calculation is equivalent to assuming an absorption cross section (κ) of about $2.9 \text{ m}^2 \text{ kg}^{-1}$ at $\lambda = 100 \mu\text{m}$. Jewitt & Matthews (1997) and Senay et al. (1998) used $\kappa = 0.05 - 0.26 \text{ m}^2 \text{ kg}^{-1}$ at 1 mm, with a $\lambda^{-\beta}$ dependence. Taking a typical β of 1 between $\lambda = 1 \text{ mm}$ and $100 \mu\text{m}$ would give $\kappa = 0.5 - 2.6 \text{ m}^2 \text{ kg}^{-1}$. We note that so long as the emissivity is close to 1 at 40–200 μm , the inferred mass is proportional to particle radius and density, so it could be rescaled for any preferred values of these parameters. With our value the ice/dust mass ratio in the beam is $\sim 0.9 - 1.2\%$ and the ratio of the cross sections is $C_i/C_d = 0.34 - 0.53$.

Dust ejected from the nucleus at an average velocity v (m s^{-1}) crosses the LWS half-beam ($1.1 \times 10^5 \text{ km}$) in a time $\tau(\text{s}) = 1.1 \times 10^8/v$. Dust tail fits between 13 and 4 AU suggest velocities of 100 m s^{-1} for 10 μm grains, with a $a^{-0.25}$ size dependence (Fulle et al. 1998). Extrapolating to 100 μm would give about 60 m s^{-1} . This is a factor of about 2 larger than terminal dust velocities calculated from Crifo & Rodionov (1997). Here we take into account Hale-Bopp nucleus size and a CO-driven coma with $Q_{\text{CO}} \sim 2 \times 10^{29} \text{ mol s}^{-1}$ (Biver et al. 1997; Crovisier et al. 1997a). Conservatively we will use $v = 60 \text{ m s}^{-1}$, which gives a travel time of $1.8 \times 10^6 \text{ s}$ (21 days). Thus to compensate for the loss of dust, the dust production rate must be equal to $Q_{\text{dust,IR}} = \frac{2}{\pi} M_{\text{dust}}/\tau = 3.9 \times 10^4 \text{ kg s}^{-1}$. This mass production rate is comparable to values estimated for small grains from visible measurements. Indeed, the dust $Af\rho$ (as defined by A'Hearn et al. 1984) was 600–2000 m at 2.9 AU (Rauer et al. 1997; Weaver et al. 1997; Schleicher et al. 1997), which corresponds to $Q_{\text{dust,vis}}$ in the range $(0.7-2.5) \times 10^4 \text{ kg s}^{-1}$ for grain radii of 1 μm and $(2.5-8.2) \times 10^4 \text{ kg s}^{-1}$ for radii of 10 μm , assuming an albedo of 0.04 and grain velocities of 300 m s^{-1} and 100 m s^{-1} , respectively. The ratio of $Q_{\text{dust,IR}}$ to $Q_{\text{dust,vis}}$ suggests a size distribution with exponent in the range 2.6–3.3 (2.8–3.6 if $v = 30 \text{ m s}^{-1}$ is assumed), in agreement with $n \leq 3.5$ derived above from the colour temperature and with measurements in P/Halley (McDonnell et al. 1991; Waniak 1992) and other comets (e.g., Hanner 1984b). The CO production rate given above corresponds to $Q_{\text{gas}} = 9.3 \times 10^3 \text{ kg s}^{-1}$ from the nucleus, hence we obtain $Q_{\text{dust,IR}}/Q_{\text{gas}} \sim 4$ (the H_2O outgassing, probably due to the sublimation of the icy grains, is not included here).

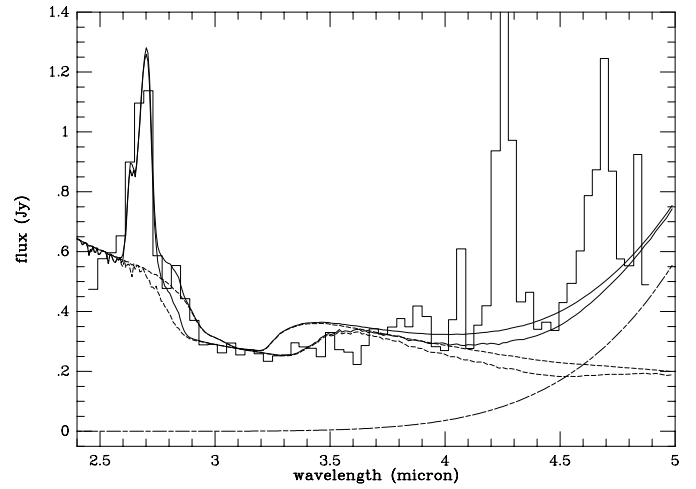


Fig. 3. The PHT-S spectrum of October 6, 1996 at 2.4–4.9 μm (histograms) along with models including reflection by dust (with constant spectral reflectance R_0) and by ice (with reflectance $R_0 e^{-\tau}$, see text), thermal emission by dust at 210 K, and emission by gaseous H_2O at 2.7 μm (calculated with $Q_{\text{H}_2\text{O}} = 3.6 \times 10^{29} \text{ s}^{-1}$ and an expansion velocity $v = 700 \text{ m s}^{-1}$ following Crovisier et al. (1997a)). Long dash – short dash: thermal component. Dashed lines: reflected component. Solid lines: sum of the two components. Thin lines are for an effective path of $l = 2 \mu\text{m}$ and thick lines for $l = 15 \mu\text{m}$

3.2. The PHT spectrum: water ice signature at 3 μm

The PHT-S data (both on 26 September and 6 October) in the 2.4–4.9 μm range indicate the presence of an absorption between 2.8 and 3.6 μm , suggestive of water ice (Fig. 3). We here focus on the 6 October data for consistency with the LWS measurements. To model this absorption, we simply assumed that the reflectivity of the ice grains is $R = R_0 e^{-\tau(\lambda)}$, where R_0 is spectrally constant and $\tau = 4\pi n'' l/\lambda$, where n'' is the imaginary refractive index of ice and l an effective absorption path. This model thus assumes that the 3 μm feature is due to absorption rather than scattering, which may not be true (see Hanner 1981). Although it is possible to calculate single scattering albedos from Mie theory for pure ice grains, such a model would not necessarily be relevant since the reflectivity of the grains is presumably considerably darkened by some mixing with dust. Indeed, for a total (dust + ice) cross section of $C_d + C_i = C = (4.3 - 4.9) \times 10^5 \text{ km}^2$, the observed flux at 2.5 μm (0.6 Jy) indicates a geometric albedo $A_g = 0.065 - 0.074$. The 2.4–4.9 μm spectrum was modelled (outside the gaseous emission bands) as the sum of a solar component (S) and a thermal component (T). The solar component, which dominates at $\lambda < 4.4 \mu\text{m}$, was fitted by the sum of a term due to the dust (constant reflectivity R_0) and a term due to the ice in the form above. S is proportional to $C R_0 (1 + K e^{-\tau})$, where K is a constant defining the relative contribution of ice and dust. Assuming that T is due to dust with a cross section C_d of $3.2 \times 10^5 \text{ km}^2$ (sublimating ice at 140–170 K contributes negligibly), the continuum at $\lambda > 4.4 \mu\text{m}$ is fitted with a dust temperature of 210 K, consistent with the analysis of the LWS data. In addition, the 2.7 μm gaseous H_2O band, which exhibits

emission wings up to $\sim 2.85 \mu\text{m}$, was included in the model. An overall fit of the PHT spectrum is shown in Fig. 3 for two values of the effective absorption path $l = 2 \mu\text{m}$ and $l = 15 \mu\text{m}$. These two models have $K = 0.6$, in qualitative agreement with $C_i/C_d = 0.34 - 0.53$ (see above). Neither of the two models gives a perfect fit to the data, which is not surprising given the extremely crude character of the models (which also neglect a possible additional thermal contribution at 3–5 μm from small hot dust grains (Williams et al. 1997)). Nevertheless, it is reassuring to find absorption paths of the order of a few μm , i.e., similar to the ice grain particle size derived from the analysis of the LWS spectrum.

4. Discussion

We have obtained evidence for water ice in the coma of comet Hale-Bopp at $r_h = 2.9$ AU and inferred a mean icy grain size of 15 μm . (We note, however, that using a single grain size is not realistic for sublimating icy grains.) Davies et al. (1997) modelled their 1.5 and 2.0 μm observations at 7 AU in terms of ice/dust mixtures (intimate or mixtures) on a solid surface (although, again, most of the flux originates from the coma). For spatial mixtures, ice particle diameters of 5–10 μm were inferred, comparable to what we find. The water ice bands were not seen in subsequent observations at 4.6 AU (Davies et al. *priv. comm.*). This is, however, not inconsistent with our detection at 2.9 AU, as the 3 μm band is much stronger than the 1.5 and 2 μm features.

Water outgassing at large r_h probably originates from icy grains in the coma. From the H_2O production rate (Fig. 3; Crovisier et al. 1997a) and our measured H_2O ice cross section and mass, we infer a grain lifetime of about 2.2 days. This is ~ 10 times longer than calculated for 15 μm grains at $T = 161$ K (Enzian 1997), indicating that this temperature is too high. The sublimation temperature can be directly estimated from $Q_{\text{H}_2\text{O}} = Z(T_s)A$, where Z is the ice sublimation rate and A , the total grain area, is equal to $4C_i$. We find $Z \sim 6 \times 10^{13} \text{ mol cm}^{-2} \text{ s}^{-1}$, i.e., $T_s \sim 153$ K at 2.9 AU. This is in very good agreement with calculations by Hanner (1981) for dirty ($n'' = 0.002$ in the visible) 15 μm icy grains.

The dust mass production rates we infer, which pertain to large ($\sim 100 \mu\text{m}$) particles, are similar to those measured for micrometre-sized particles in the visible at the same r_h . Dust production rates have similarly been determined from millimetre/submillimetre measurements performed near perihelion (Senay et al. 1998; Wink et al. 1998). Although these determinations are uncertain because the appropriate dust velocity is poorly known, they also suggest that large particles importantly contribute to (or even dominate) the mass of the dust coma.

Acknowledgements. We are indebted to M. Combi, M. Fulle, and L. Jorda for enlightening discussions

References

- A'Hearn, M.F., Schleicher, D.G., Feldman, P.D., Millis, R.L., Thompson, D.T., 1984, *AJ* 89, 579
- Biver, N., Bockelée-Morvan, D., Colom, P., et al., 1997, *Sci* 275, 1915
- Clegg, P.E., Ade, P.A.R., Armand, C., et al., 1996, *A&A* 315, L38
- Crifo, J.F., Rodionov, A.V., 1997, *Icarus* 127, 319
- Crovisier, J., Leech, K., Bockelée-Morvan, D., et al., 1997a, *Sci* 275, 1904
- Crovisier, J., Leech, K., Bockelée-Morvan, D., et al., 1997b, *ESA SP-419*, 137
- Dartois, E., Cox, P., Roelfsema, P.R., et al., 1998, *A&A* 338, L21
- Davies, J.K., Roush, T.L., Cruikshank, D.P., et al., 1997, *Icarus* 127, 238
- Delsemme, A.H., Miller, D.C., 1971, *Planet. Space Sci.* 19, 1229
- Enzian, A., 1997, PhD thesis, Université Joseph Fourier, Grenoble
- Enzian, A., Cabot, H., Klinger, J., 1998, *Planet. Space Sci.* (in press)
- Fulle, M., Cremonese, G., Böhm, C., 1998, *AJ* 116, 1470
- Hanner, M.S., 1981, *Icarus* 47, 342
- Hanner, M.S., 1984a, *ApJ* 277, L75
- Hanner, M.S., 1984b, *Adv. Space Res.* 4, 189
- van de Hulst, H.C., 1957, *Light Scattering by Small Particles*, John Wiley & Sons, Inc., N.Y.
- Jewitt, D.J., Matthews, H.E., 1997, *AJ* 113, 1145
- Koike, C., Shibai, H., 1998, ISAS report 671
- Koike, C., Shibai, H., Tsuchiyama, A., 1993, *MNRAS* 264, 654
- Lemke, D., Klaas, U., Abolins, J., et al., 1996, *A&A* 315, L64
- McDonnell, J.A.M., Lamy, P.L., Pankiewicz, G.S., 1991, in *Comets in the Post-Halley Era* (eds R.L. Newburn, M. Neugebauer and J. Rahe), Kluwer, Dordrecht, 1043
- Malfait, K., Waelkens, C., Waters, L.B.F.M., et al., 1998, *A&A* 332, L25
- Omont, A., Moseley, S.H., Forveille, T., et al., 1990, *ApJ* 355, L27
- Prialnik, D., 1998, *Earth Moon and Planets* (in press)
- Rauer, H., Arpigny, C., Boehnhardt, H., et al., 1997, *Sci* 275, 1909
- Schleicher, D.G., Lederer, S.M., Millis, R.L., et al., 1997 *Sci* 275, 1913
- Senay, M., Rownd, B., Dickens, J.E., et al., 1998, in *The First International Conference on Comet Hale-Bopp*, Tenerife, Spain
- Trotta, F., 1996, PhD thesis, Université Joseph Fourier, Grenoble
- Waniak, W., 1992, *Icarus* 100, 154.
- Weaver, H.A., Feldman, P.D., A'Hearn, M.F., et al., 1997, *Sci* 275, 1900
- Weaver, H.A., Lamy, P., 1998, *Earth Moon and Planets* (in press)
- Williams, D.M., Mason, C.G., Gehr, R.D., et al., 1997, *ApJ* 489, L91
- Wink, J., Altenhoff, W.J., Biegging, J., et al., 1998, in *The First International Conference on Comet Hale-Bopp*, Tenerife, Spain
- Wooden, D.H., Harker, D.E., Woodward, C.E., et al., 1998, *ApJ* (in press)